



Published in final edited form as:

Ophthalmol Glaucoma. 2022 ; 5(6): 572–580. doi:10.1016/j.ogla.2022.05.004.

Multi-Pressure Dial Goggle Effects on Circumpapillary Structure and Microvasculature in Glaucoma Patients

Alireza Kamalipour, MD, MPH^{1,*}, Sasan Moghimi, MD^{1,*}, Veronica R. Inpirom¹, Golnoush Mahmoudinezhad, MD, MPH¹, Robert N. Weinreb, MD¹

¹Hamilton Glaucoma Center, Shiley Eye Institute, Viterbi Family Department of Ophthalmology, University of California San Diego, La Jolla, CA.

Abstract

Purpose—To evaluate the effects of Multi-Pressure Dial (MPD) induced pressure changes on circumpapillary retinal nerve fiber layer (RNFL) and capillary density (CD) measurements in glaucoma patients using Optical Coherence Tomography Angiography (OCTA).

Design—Prospective interventional study

Participants—Twenty-four patients with primary open angle glaucoma

Methods—One eye of each patient underwent negative pressure application with the MPD. The MPD alters intraocular pressure (IOP) relative to atmospheric pressure by generating a negative pressure vacuum within a goggle chamber that is placed over the eye. Each participant underwent serial HD OCTA imaging (Angiovue) of the optic nerve head at different negative pressure increments of 5 mmHg, starting from 0 mmHg to 20 mmHg and then returning to baseline. Images were acquired after 2 minutes of sustained negative pressure at each target pressure to allow for stabilization of the retinal structures and microvasculature. RNFL thickness and CD measurements were automatically calculated using the native Angiovue software and then exported for analysis.

Main Outcome Measures—The influence of different levels of negative pressure on circumpapillary RNFL thickness and CD measurements assessed by a linear mixed effects model with repeated measures.

Results—Mean (\pm SD) age was 71.0 (\pm 7.8) years, baseline IOP was 17.5 (\pm 3.6) mmHg, and there was a mean 24–2 mean deviation of -2.80 (\pm 2.55) dB. Serial circumpapillary CD measurements showed a statistically significant dose-dependent increase from baseline without negative pressure application to the maximum negative pressure application of 20 mmHg [difference: 2.27%, $P = 0.010$]. CD measurements then decreased symmetrically when lowering the negative pressure to baseline. Circumpapillary CD measurements at target negative pressures of 10 mmHg, 15 mmHg, and 20 mmHg were significantly higher than the baseline measurements (all $P < 0.05$). Circumpapillary RNFL thickness remained the same throughout different levels of negative pressure.

Correspondence: Robert N. Weinreb, MD, Shiley Eye Institute, University of California, San Diego, 9500 Gilman Drive, La Jolla, CA 92093-0946. rweinreb@ucsd.edu.

*These authors had equal contributions as co-first authors.

Conclusions—Circumpapillary CD measurements showed a dose-dependent increase with the induction of negative pressure while RNFL thickness measurements remained unchanged.

Precis:

This study found that circumpapillary capillary density shows a dose-response increase after the induction of negative periocular pressure using multi-pressure dial while retinal nerve fiber layer thickness remains unchanged.

Keywords

optical coherence tomography angiography; multi-pressure dial; IOP; glaucoma

Introduction

Glaucoma is characterized by progressive damage to the retinal ganglion cells along with commensurate visual field (VF) loss.^{1, 2} The alteration and impairment of ocular circulation in glaucoma has been well documented using various modalities including color doppler imaging, laser speckle flowgraphy and, more recently, optical coherence tomography angiography (OCTA).^{3–13} The advent of OCTA has provided a unique opportunity for high resolution quantitative evaluation of retinal microvasculature in a non-invasive manner.^{14, 15} Numerous studies have demonstrated the utility of OCTA for the diagnosis of glaucoma, and also for the assessment of glaucoma progression.^{16–25}

The high correlation between OCT and OCTA derived metrics^{25, 26} have led to some questions about whether OCTA measurements improve or complement structural OCT parameters for the management of glaucoma. Therefore, recent studies have evaluated the possible complementary role of OCTA and OCT measurements for diagnosis,^{25, 27} the structure-function relationship,^{25, 28, 29} and monitoring of disease progression^{20, 24, 30} in glaucoma patients. OCTA has the potential to evaluate changes related to the inherent dynamic nature of retinal microcirculation and the potential effects of autoregulation and intraocular pressure (IOP) fluctuations. However, it is not known clearly whether OCTA can evaluate these short-term dynamic alterations or whether it simply adds another “static” structural component similar to those already provided by OCT. Lack of an appropriate experimental design for changing human IOP in a controlled fashion that is compatible with the working principles of OCTA technology has been a barrier toward understanding this.

The multi-pressure dial system (MPD; Equinox Ophthalmic, Inc., CA, USA) is a recently developed technology that has been proposed for non-invasive IOP reduction in a controlled adjustable fashion.^{31–34} It consists of a pair of pressure-sensing goggles that individually seal both periorbital regions with separate connections to a pressure-modulating pump on each side.^{31, 33, 35} Once the goggles are appropriately fitted, target negative pressure can be adjusted via software to an individualized pressure at each periorbital region. The working principles of this technology have previously been described.³⁵

Previous studies using the MPD have evaluated its short-term safety, tolerability and its effectiveness in reducing IOP relative to atmospheric pressure. For safety and tolerability

images (described later), physical inability to be properly positioned at the imaging devices or eye exam equipment, a previous history of glaucoma related filtering surgery, including trabeculectomy and tube-shunt procedures, and a known history of allergy to silicone (MPD goggle seals are made of silicone) were excluded from the study. Participants were also excluded if they had a diagnosis of Parkinson's disease, Alzheimer's disease, dementia, or a history of stroke. After completion of the ophthalmological examination, the eye with worse glaucomatous damage based on Hodapp-Parrish-Anderson Criteria³⁷ was selected for subsequent OCTA imaging.

Multi-Pressure Dial system and imaging protocol

For this study, the MPD system was used to generate and maintain precise levels of negative periocular pressure for 2 minutes before OCTA image acquisition. The overall design of this system is previously described.^{31, 33} In brief, it consists of goggles that seal each periocular chamber and are separately connected to a pressure sensor that can adjust pressure independently on each side to a specific targeted value (Figure 1-A). OCTA imaging at different levels of negative pressure was performed without any interruption in negative pressure while the goggles were on the patients. The imaging protocol is described next in detail. To mitigate the potential effect of condensations within the sealed goggle chambers on OCTA image quality, two small holes were drilled on the most medial region of each goggle (Figure 1-B) for a controlled leak. Moreover, the front surface of the goggles was continuously monitored for condensation. The lens clarity was assessed and confirmed throughout the imaging session. During each imaging session, the periocular pressure was continuously monitored using the Equinox native software that receives real-time input signal from the pressure sensor (Figure 2). Accordingly, prior to each imaging session for each negative pressure level, it was confirmed that 2 minutes of uninterrupted negative target pressure was sustained according to the imaging protocol. Images were reacquired in case of any compromise to the protocol.

Prior to negative pressure application, the OCTA imaging protocol included a baseline measurement of the study eye with the MPD system. Subsequent images were obtained at different negative pressure levels following a "ramp-up" and a "ramp-down" schedule, and then finally without negative pressure once again to complete the imaging series (Table 1). In brief, the subsequent OCTA images were taken at baseline pressure (0 mmHg), level 1 (-5 mmHg), level 2 (-10 mmHg), level 3 (-15 mmHg), level 4 (-20 mmHg), level 5 (-15 mmHg), level 6 (-10 mmHg), level 7 (-5 mmHg), and level 8 (0 mmHg). The target negative pressure at different levels was continuously monitored and remained unchanged during imaging, and images were acquired after a two-minute interval at each level to allow for stabilization of the measurements. If negative pressure application was interrupted at any time, the negative pressure was programmed to the prior setting and the minimum timing sequence was re-initiated. For example, if negative pressure application was interrupted during -20 mmHg, the negative pressure was set to -15 mmHg and the minimum two-minute period was re-initiated prior to increasing negative pressure to -20 mmHg. The OCTA imaging series was conducted once in each patient.

Spectral-Domain OCT and OCT Angiography

Spectral-domain OCT and OCTA imaging of the macula were performed the AngioVue imaging system (Optovue, Inc., Fremont, CA, USA, Version 2018,1,1,63). With this platform, Spectral-domain OCT and OCTA images are obtained from the same volumetric scans. This allows precise automated registration of OCT and OCTA images and provides quantified metrics for the analysis of the layer of interest.

We analyzed capillary density (CD) at the radial peripapillary capillary plexus derived from HD OCTA volume scans comprised of 400×400 A-scans with a 4.5×4.5 mm² field of view centered on the optic disc. Angiovue split-spectrum amplitude-decorrelation angiography was used to capture the dynamic motion of the red blood cells and provide a high-resolution 3-dimensional visualization of perfused retinal microvasculature. Capillary density measurements were calculated as the percent area occupied by flowing blood vessels in the region of interest after the automated removal of large vessels from the original en-face angiogram using the Angiovue software. The retinal layers of each scan were automatically segmented by the AngioVue software in order to visualize the radial peripapillary capillary plexus layer in a slab from internal limiting membrane to RNFL posterior boundary. Circumpapillary CD measurements were calculated over the region defined as a 750- μ m-wide elliptical annulus extending from the optic disc boundary encircling 360-degree global area. Similarly, hemifield measurements were obtained using the entire corresponding hemifield in each image. The same volume scan used for analysis of circumpapillary CD measurements derived from OCTA en-face images was used to measure the circumpapillary RNFL thickness. Global average and the corresponding hemifield RNFL thickness measurements were analyzed based on the same retinal slab boundaries used for the OCTA CD measurements.

Only good-quality images were included in the analysis. Image quality review was completed on all OCTA and OCT images processed with standard AngioVue software (version 2018,1,1,63) according to a previously reported protocol that evaluates for the presence of different types of OCTA artifacts.³⁸ An expert reviewer evaluated all of the images and excluded those with poor quality, briefly defined as images with any of the following: (1) low scan quality with quality index of less than 4, (2) defocus, (3) residual motion artifacts visible as irregular vessel pattern or disc boundary on the en-face angiogram, (4) image cropping or local weak signal resulting from vitreous opacity, (5) signal devoid area as a result of blink, (6) poor centration on the fovea and (7) the presence of segmentation errors that could not be corrected.³⁸

Statistical Analysis

Continuous and categorical data are presented as mean (95% confidence interval [CI]) and counts (%). Linear mixed model with repeated measures was used to assess the effect of different levels of negative pressure on circumpapillary RNFL thickness and CD measurements. Different levels of negative pressure were treated as repeated observations in this model.³⁹ Due to the exploratory nature of this analysis, no type I error correction for multiple comparisons was applied as recommended by Bender and Lange.⁴⁰ Separate subanalyses were performed after adjustment for the effects of age and OCTA signal

strength index (SSI) in the models. Statistical analysis was performed using Stata software version 17.0 (StataCorp, College Station, TX). P -value < 0.05 was considered as statistically significant.

Results

One eye from each of 24 glaucoma patients were included in this prospective open label clinical trial. The mean age of participants was 71.0 years (67.7, 74.2) and the majority were females ($n = 13$, 54%) and Caucasian ethnicity ($n = 18$, 75%). There was an average mean deviation (MD) of -2.80 dB (-3.88 , -1.72) and PSD of 3.99 dB (2.60, 5.38). The overall demographic and ocular characteristics of the study participants are shown in Table 2. The majority of patients ($N = 15$, 63%) were on ocular hypotensive treatment at the time of study participation including prostaglandin agonists ($N = 13$, 54%), β -blockers ($N = 6$, 24%), α_2 agonists ($N = 2$, 8%), and carbonic anhydrase inhibitors ($N = 2$, 8%). Using the MPD goggles after creating small holes, there was no evidence of any condensation over the front surface of the goggles during the image acquisition procedure. Therefore, there was no need to clean the goggles, and the periocular vacuum remained uninterrupted throughout the imaging sequence for all study participants. After OCTA image quality evaluation, 189 out of 216 captured images (87.5%) were included in the analysis. Poor-quality images ($N = 27$, 12.5%) were excluded due to the presence of OCTA artifacts including motion ($N = 22$, 81.5%), defocus ($N = 20$, 74.1%), segmentation error ($N = 11$, 40.7%), poor centration ($N = 11$, 40.7%), image cropping ($N = 9$, 33.3%), and local weak signal ($N = 2$, 7.4%).

Mean circumpapillary RNFL thickness and CD at baseline negative pressure (0 mmHg) were 77.68 μm (71.95, 83.40) and 41.84 % (39.06, 44.61), respectively. Table 3 shows the changes in circumpapillary RNFL thickness and CD compared to the baseline measurements at different levels of negative pressure. No statistically significant difference was observed in serial measurements of circumpapillary RNFL thickness at different levels of negative pressure compared to the baseline (all P -values > 0.05). However, circumpapillary CD measurements showed a symmetric increase compared to the baseline values at different levels of negative pressure. During the “ramp-up” schedule, circumpapillary CD showed a statistically significant increase from the baseline value at the negative pressure levels of -10 mmHg (1.74%, P -value = 0.042), -15 mmHg (1.77%, P -value = 0.042), and -20 mmHg (2.27%, P -value = 0.010). Similarly, during the “ramp-down” schedule, the differences of circumpapillary CD from the baseline value remained statistically significant at the negative pressure levels of -15 mmHg (2.05%, P -value = 0.014), and -10 mmHg (1.92%, P -value = 0.021). The maximum increase in circumpapillary CD was observed at a negative pressure setting of 20 mmHg with the absolute value of 2.27 % (0.54, 4.01) that corresponded to a relative increase of 5.43 % from the baseline measurements [Figure 3]. Separate analysis after adjusting for age and SSI at different levels of negative pressure revealed similar findings (Supplemental Table 1). In secondary data analysis, we found no statistically significant linear association between MD and circumpapillary CD changes at different levels of negative pressure (all P -values > 0.05) [Supplemental Table 2].

Supplemental analyses at the superior (Table 4) and inferior (Table 5) hemifield levels revealed similar findings to those of global measurements. Circumpapillary RNFL thickness

remained stable at different levels of negative pressure in both superior and inferior hemifields. At the superior hemifield, circumpapillary CD showed a statistically significant increase from the baseline value at the negative pressure levels of -10 mmHg (during ramp-down, 2.06%, P -value = 0.014), -15 mmHg (during ramp-down, 1.99%, P -value = 0.018), and -20 mmHg (1.95%, P -value = 0.029). At the inferior hemifield, circumpapillary CD showed a statistically significant increase from the baseline value at the negative pressure levels of -10 mmHg (during ramp-up, 2.11%, P -value = 0.037), -15 mmHg (during ramp-down, 2.10%, P -value = 0.036), and -20 mmHg (2.44%, P -value = 0.020). Notably, the superior and inferior hemifields showed 4.62% and 5.89% relative percentages of increase from their corresponding baseline measurements at a negative pressure setting of 20 mmHg, respectively (Figure 3). Separate analyses revealed that various levels of negative pressure during the “ramp-up” and “ramp-down” schedule did not have a statistically significant influence on the difference between the superior and inferior hemifield RNFL thickness and CD measurements (Supplemental Table 3).

Discussion

In the current study, we investigated the alterations of circumpapillary RNFL thickness and microvasculature while using the MPD to generate and maintain graded negative periorcular pressure. Our findings indicate that circumpapillary RNFL thickness remains stable while circumpapillary CD increases (as much as 5.4% of the baseline values at -20 mmHg) during the short-term application of negative periorcular pressure using the MPD. Notably, separate analyses at each hemifield level revealed similar patterns of change in circumpapillary RNFL thickness and CD after inducing negative pressure. These findings demonstrate that retinal microcirculation is increased with MPD induced negative pressure.

The current study showed that increased circumpapillary CD measurements had a dose dependent relationship with the magnitude of negative periorcular pressure. Similar changes of mean circumpapillary CD relative to baseline values without application of negative pressure were observed at each target negative periorcular pressure. The gradual increase in circumpapillary CD during “ramp-up” of negative pressure was similar to the gradual reduction in circumpapillary CD during the “ramp-down” of negative pressure. These changes were observed not only based on global measurements, but also at the hemifield level even when adjusted for the OCTA signal strength. No significant changes were observed in circumpapillary RNFL thickness at different negative pressure levels despite using the same segmentation boundaries and measurement regions derived from the same volume scans used for circumpapillary CD measurements.

OCTA has provided insight into the role of microvascular damage in diagnosing and management of glaucoma^{16, 21, 25, 41}, as well as the association of microvascular measurements with disease progression.^{19, 24, 42} However, it remains unknown whether OCTA measurements are clinically useful to detect short-term dynamic alterations of retinal microcirculation resulting from changes in IOP or due to autoregulation. The technical limitations partly explain this gap for the assessment of such responses in a controlled setting. The findings of two recent studies show promise to support the utility of OCTA measurements for detecting short-term dynamic microvascular alterations. Fan et al. showed

that OCTA measured circumpapillary microvascular parameters decline with response to hyperoxia.⁴³ In addition, Liu and associates found that macular OCTA microvascular assessments decrease after reducing cerebrospinal fluid pressure.⁴⁴ As MPD modulates IOP in a graded fashion based on the level of negative periocular pressure,³² the current study is the first to demonstrate that OCTA also can detect short-term dynamic alterations of retinal microcirculation resulting from changes in IOP. This supports a complementary and potentially additive role for the assessments provided by OCTA relative to OCT-based RNFL thickness measurements. The combination of using the MPD to generate and maintain negative periocular pressure and using OCTA to capture images in real time during negative pressure application provides an opportunity to gain deeper insight on how changes in IOP and possible autoregulatory mechanisms affect retinal microcirculation in healthy individuals and glaucoma patients.

The induction of negative periocular pressure was followed by increased circumpapillary microvascular circulation. A previous study used an existing validated lumped-parameter model of the eye to describe the dynamic alterations of IOP, episcleral venous pressure, aqueous humor and total globe volume, and ocular blood flow after generation and maintenance of negative periocular pressure. The authors concluded that the induction of negative periocular pressure leads to a relatively rapid reduction in IOP accompanied by an increase in the total ocular blood flow and suggested different ocular characteristics, including aqueous humor dynamics, episcleral venous pressure, and tissue dampening effects affect the target IOP reduction.³⁵ Although the utilized model was limited in representing a complex system by just a few compartments, their model predictions were consistent with the in-vivo observations of the present study. The MPD goggles used in the mentioned study did not contain the holes that we created for the imaging purposes of the present study. The MPD goggles' working principle relies on creating and maintaining negative inside-the-goggle pressure. This pressure was constantly monitored in real-time using a pressure sensor inside the goggle chamber. It was ensured that the time sequence and the target pressure level remain consistent with the protocol for all participants throughout the study. Therefore, the holes had no impact on the MPD goggles' performance for the currently investigated ranges of negative pressure. The plausibility of the pathophysiologic mechanism and the symmetry and apparent graded dose-response shape of changes in microcirculation over successive levels of negative pressure support the hypothesis that short-term generation and maintenance of negative periocular pressure proportionately increases ocular microcirculation, albeit over a limited range of negative pressure used for this study. Whether or not this measurable, quantifiable change in retinal microcirculation provides a diagnostic or therapeutic advantage in the management of glaucoma remains to be addressed by future studies.

The dependence of OCTA-measured retinal microcirculation on IOP reduction might have clinical implications in glaucoma patients.⁴⁵⁻⁴⁸ Liu and colleagues⁴⁵ evaluated 17 glaucoma patients six months after surgical IOP reduction and found evidence of increased ONH microcirculation, especially in minimally damaged RNFL regions. At the same time, no apparent change was observed in RNFL thickness indicating that such alterations are unlikely to be captured by OCT-provided metrics since RNFL thinning indicates cell loss that is deemed theoretically irreversible.⁴⁵ Moreover, two other studies demonstrated

increased retinal microcirculation at the circumpapillary⁴⁷ and the macular⁴⁶ areas three months after surgical IOP reduction. Notably, all of the aforementioned improvements in retinal microcirculation were detected months after IOP reduction. These observations suggest the possibility of a gradual metabolic recovery of damaged, but viable, retinal ganglion cells that might also be responsive to treatment after IOP is lowered.⁴⁵ We speculate that the evaluation of short-term microvascular changes resulting from presumed IOP reduction might be useful for risk assessment in patients who are glaucoma suspects or those with existing disease. It might also be used as a screening modality to evaluate potential candidates of IOP lowering therapy.

The present study has several limitations. First, the OCTA images were acquired after a two-minute interval at each target pressure to allow for stabilization of the measurements. However, the potential autoregulatory response and the resultant microvascular changes might differ over more prolonged intervals. Also, a time-dependent response at the same level of negative pressure might exist that could be captured by repeated measurements, all opportunities for future studies. Second, the present study included a limited range of negative target pressure. Thus, caution must be made in generalizing the results to negative periocular pressures outside this range. Third, adjusting the periocular borders of the goggles to tightly control the negative target pressure was challenging in a few patients because of individualized anatomical features. Nevertheless, we did manage to monitor even fine alterations of pressure outside the target level using the computer software, ensuring all measurements were obtained according to the protocol. Unfortunately, we were unable to obtain good quality macular images, perhaps due to the goggles interfering with the tracking system of the OCTA instrument for the macular scan protocol. Evaluation of macular ganglion cell complex thickness and vessel density change at different levels of negative pressure remains an item for future investigations. Also, the level of IOP was unknown at the time of OCTA imaging in the present study. It should be noted that a majority of patients were on ocular hypotensive treatment at the time of study participation. The effect of ocular hypotensive medications on retinal vascular reactivity in glaucoma is not currently well established. Most available studies have evaluated homeostatic hemodynamic parameters, rather than assessing hemodynamic response to a provocation,⁴⁹ as done in the current study. And last, as previously reported, artifacts with the potential influence on the instrument metrics are frequent.³⁸ Accordingly, all acquired OCTA images were manually reviewed for the presence of different OCTA artifacts,³⁸ and only good-quality images were included in the final analysis.

In conclusion, the combination of the MPD with OCTA quantifies retinal microvascular alterations in response to presumed changes in IOP. There was increased retinal microcirculation consistent with the magnitude of negative MPD pressure, possibly resulting from graded IOP reduction. In contrast to the changes in microcirculation, RNFL thickness measurements remained stable at all negative pressure levels.

Supplementary Material

Refer to Web version on PubMed Central for supplementary material.

Acknowledgement:

Financial Support:

National Institutes of Health/National Eye Institute Grants R01EY029058, R01EY011008, U10EY014267, R01EY026574, R01EY019869 and R01EY027510; Core Grant P30EY022589; an unrestricted grant from Research to Prevent Blindness (New York, NY); UC Tobacco- Related Disease Research Program (T31IP1511); and grants for participants' glaucoma medications from Alcon, Allergan, Pfizer, Merck, and Santen.

Commercial Disclosures:

1. Alireza Kamalipour: none
2. Sasan Moghimi: none
3. Veronica R. Inpirom: none
4. Golnoush Mahmoudinezhad: none
5. Robert N. Weinreb: Financial support (research instruments) - Heidelberg Engineering, Carl Zeiss Meditec, Konan Medical, Optovue, Centervue, Bausch & Lomb; Consultant - Abbvie, Aerie Pharmaceuticals, Equinox, Eyenovia; Patent - Toromedes, Carl Zeiss Meditec.

Abbreviations and Acronyms:

BCVA	best-corrected visual acuity
CCT	central corneal thickness
CD	capillary density
D	diopter
IOP	intraocular pressure
MD	mean deviation
MPD	multi-pressure dial
OCTA	optical coherence tomography angiography
ONH	optic nerve head
PSD	pattern standard deviation
RNFL	retinal nerve fiber layer thickness
SD-OCT	spectral domain-OCT
SSI	signal strength index
VF	visual field

References

1. Weinreb RN, Aung T, Medeiros FA. The pathophysiology and treatment of glaucoma: a review. *Jama* 2014;311:1901–11. [PubMed: 24825645]
2. Weinreb RN, Leung CK, Crowston JG, et al. Primary open-angle glaucoma. *Nature reviews Disease primers* 2016;2:16067.
3. Weinreb RN, Harris A. *Ocular blood flow in glaucoma*: Kugler Publications, 2009.

4. Flammer J, Orgül S, Costa VP, et al. The impact of ocular blood flow in glaucoma. 2002;21:359–393.
5. Zeitz O, Galambos P, Wagenfeld L, et al. Glaucoma progression is associated with decreased blood flow velocities in the short posterior ciliary artery. 2006;90:1245–1248.
6. Moore NA, Harris A, Wentz S, et al. Baseline retrobulbar blood flow is associated with both functional and structural glaucomatous progression after 4 years. 2017;101:305–308.
7. Schmidl D, Garhofer G, Schmetterer L. The complex interaction between ocular perfusion pressure and ocular blood flow - relevance for glaucoma. *Experimental eye research* 2011;93:141–55. [PubMed: 20868686]
8. Plange N, Kaup M, Arend O, Remky A. Asymmetric visual field loss and retrobulbar haemodynamics in primary open-angle glaucoma. *Graefe's archive for clinical and experimental ophthalmology = Albrecht von Graefes Archiv fur klinische und experimentelle Ophthalmologie* 2006;244:978–83.
9. Zeitz O, Galambos P, Wagenfeld L, et al. Glaucoma progression is associated with decreased blood flow velocities in the short posterior ciliary artery. *Br J Ophthalmol* 2006;90:1245–8. [PubMed: 16825276]
10. Kuerten D, Fuest M, Koch EC, Koutsonas A, Plange N. Retrobulbar Hemodynamics and Visual Field Progression in Normal Tension Glaucoma: A Long-Term Follow-Up Study. *BioMed research international* 2015;2015:158097. [PubMed: 26557652]
11. Martínez A, Sánchez M. Predictive value of colour Doppler imaging in a prospective study of visual field progression in primary open-angle glaucoma. *Acta ophthalmologica Scandinavica* 2005;83:716–22. [PubMed: 16396650]
12. Galassi F, Nuzzaci G, Sodi A, Casi P, Cappelli S, Vielmo A. Possible correlations of ocular blood flow parameters with intraocular pressure and visual-field alterations in glaucoma: a study by means of color Doppler imaging. *Ophthalmologica Journal international d'ophthalmologie International journal of ophthalmology Zeitschrift fur Augenheilkunde* 1994;208:304–8.
13. Kiyota N, Shiga Y, Yasuda M, et al. Sectoral Differences in the Association of Optic Nerve Head Blood Flow and Glaucomatous Visual Field Defect Severity and Progression. *Invest Ophthalmol Vis Sci* 2019;60:2650–2658. [PubMed: 31226712]
14. Mansouri KJ, Erond. Optical coherence tomography angiography and glaucoma: searching for the missing link. 2016;13:879–880.
15. Jia Y, Tan O, Tokayer J, et al. Split-spectrum amplitude-decorrelation angiography with optical coherence tomography. 2012;20:4710–4725.
16. Yarmohammadi A, Zangwill LM, Diniz-Filho A, et al. Optical Coherence Tomography Angiography Vessel Density in Healthy, Glaucoma Suspect, and Glaucoma Eyes. *Investigative Ophthalmology & Visual Science* 2016;57:OCT451–OCT459. [PubMed: 27409505]
17. Yarmohammadi A, Zangwill LM, Diniz-Filho A, et al. Relationship between Optical Coherence Tomography Angiography Vessel Density and Severity of Visual Field Loss in Glaucoma. *Ophthalmology* 2016;123:2498–2508. [PubMed: 27726964]
18. Moghimi S, Zangwill LM, Penteado RC, et al. Macular and Optic Nerve Head Vessel Density and Progressive Retinal Nerve Fiber Layer Loss in Glaucoma. *Ophthalmology* 2018;125:1720–1728. [PubMed: 29907322]
19. Shin JW, Song MK, Kook MS. Association Between Progressive Retinal Capillary Density Loss and Visual Field Progression in Open-Angle Glaucoma Patients According to Disease Stage. *American Journal of Ophthalmology* 2021;226:137–147. [PubMed: 33524366]
20. Hou H, Moghimi S, Proudfoot JA, et al. Ganglion Cell Complex Thickness and Macular Vessel Density Loss in Primary Open-Angle Glaucoma. *Ophthalmology* 2020;127:1043–1052. [PubMed: 32085875]
21. WuDunn D, Takusagawa HL, Sit AJ, et al. OCT Angiography for the Diagnosis of Glaucoma: A Report by the American Academy of Ophthalmology. *Ophthalmology* 2021;128:1222–1235. [PubMed: 33632585]
22. Kim J-A, Lee EJ, Kim T-W. Evaluation of Parapapillary Choroidal Microvasculature Dropout and Progressive Retinal Nerve Fiber Layer Thinning in Patients With Glaucoma. *JAMA ophthalmology* 2019;137:810–816. [PubMed: 31120486]

23. Yarmohammadi A, Zangwill LM, Manalastas PIC, et al. Peripapillary and Macular Vessel Density in Patients with Primary Open-Angle Glaucoma and Unilateral Visual Field Loss. *Ophthalmology* 2018;125:578–587. [PubMed: 29174012]
24. Kamalipour A, Moghimi S, Hou H, et al. Multilayer Macula Vessel Density and Visual Field Progression in Glaucoma. *American Journal of Ophthalmology* 2021.
25. Kamalipour A, Moghimi S, Jacoba CM, et al. Measurements of OCT Angiography Complement OCT for Diagnosing Early Primary Open-Angle Glaucoma. *Ophthalmology Glaucoma* 2021.
26. Yarmohammadi A, Zangwill LM, Diniz-Filho A, et al. Relationship between Optical Coherence Tomography Angiography Vessel Density and Severity of Visual Field Loss in Glaucoma. *Ophthalmology* 2016;123:2498–2508. [PubMed: 27726964]
27. Rabiolo A, Fantaguzzi F, Sacconi R, et al. Combining Structural and Vascular Parameters to Discriminate Among Glaucoma Patients, Glaucoma Suspects, and Healthy Subjects. *Transl Vis Sci Technol* 2021;10:20.
28. Wong D, Chua J, Lin E, et al. Focal Structure-Function Relationships in Primary Open-Angle Glaucoma Using OCT and OCT-A Measurements. *Invest Ophthalmol Vis Sci* 2020;61:33.
29. Wong D, Chua J, Tan B, et al. Combining OCT and OCTA for Focal Structure-Function Modeling in Early Primary Open-Angle Glaucoma. *Invest Ophthalmol Vis Sci* 2021;62:8.
30. Hou H, Moghimi S, Kamalipour A, et al. Macular Thickness and Microvasculature Loss in Glaucoma Suspect Eyes. *Ophthalmology Glaucoma* 2021.
31. Thompson VM, Ferguson TJ, Ahmed IIK, et al. Short-Term Safety Evaluation of a Multi-Pressure Dial: A Prospective, Open-label, Non-randomized Study. *Ophthalmology and therapy* 2019;8:279–287. [PubMed: 30919318]
32. Swan RJ, Ferguson TJ, Shah M, et al. Evaluation of the IOP-Lowering Effect of a Multi-Pressure Dial at Different Negative Pressure Settings. *Transl Vis Sci Technol* 2020;9:19.
33. Samuelson TW, Ferguson TJ, Radcliffe NM, et al. 8 hrs Safety Evaluation Of A Multi-Pressure Dial In Eyes With Glaucoma: Prospective, Open-Label, Randomized Study. *Clinical ophthalmology (Auckland, NZ)* 2019;13:1947–1953.
34. Ferguson TJ, Radcliffe NM, Van Tassel SH, et al. Overnight Safety Evaluation of a Multi-Pressure Dial in Eyes with Glaucoma: Prospective, Open-Label, Randomized Study. *Clinical ophthalmology (Auckland, NZ)* 2020;14:2739–2746.
35. Ethier CR, Yoo P, Berdahl JP. The effects of negative periocular pressure on intraocular pressure. *Experimental eye research* 2020;191:107928. [PubMed: 31926968]
36. Goldberg JL, Jimenez-Roman J, Hernandez-Oteyza A, Quiroz-Mercado H. Short-term Evaluation of Negative Pressure Applied by the Multi-Pressure Dial System to Lower Nocturnal IOP: A Prospective, Controlled, Intra-subject Study. *Ophthalmology and therapy* 2021;10:349–358. [PubMed: 33871812]
37. Hodapp E, Parrish RK, Anderson DR. *Clinical decisions in glaucoma*: Mosby Incorporated, 1993.
38. Kamalipour A, Moghimi S, Hou H, et al. OCT Angiography Artifacts in Glaucoma. *Ophthalmology* 2021.
39. Detry MA, Ma YJJ. Analyzing repeated measurements using mixed models. 2016;315:407–408.
40. Bender R, Lange S. Adjusting for multiple testing--when and how? *Journal of clinical epidemiology* 2001;54:343–9. [PubMed: 11297884]
41. Jia Y, Wei E, Wang X, et al. Optical coherence tomography angiography of optic disc perfusion in glaucoma. 2014;121:1322–1332.
42. Moghimi S, Zangwill LM, Pentead RC, et al. Macular and optic nerve head vessel density and progressive retinal nerve fiber layer loss in glaucoma. 2018;125:1720–1728.
43. Fan X, Xu H, Zhai R, Sheng Q, Kong X. Retinal Microcirculatory Responses to Hyperoxia in Primary Open-Angle Glaucoma Using Optical Coherence Tomography Angiography. *Invest Ophthalmol Vis Sci* 2021;62:4.
44. Liu X, Khodeiry MM, Lin D, et al. The association of cerebrospinal fluid pressure with optic nerve head and macular vessel density. *Science China Life sciences* 2021.

45. Liu L, Takusagawa HL, Greenwald MF, et al. Optical coherence tomographic angiography study of perfusion recovery after surgical lowering of intraocular pressure. *Sci Rep* 2021;11:17251. [PubMed: 34446739]
46. Shoji T, Kanno J, Weinreb RN, et al. OCT angiography measured changes in the foveal avascular zone area after glaucoma surgery. *Br J Ophthalmol* 2022;106:80–86. [PubMed: 33153992]
47. Shin JW, Sung KR, Uhm KB, et al. Peripapillary Microvascular Improvement and Lamina Cribrosa Depth Reduction After Trabeculectomy in Primary Open-Angle Glaucoma. *Invest Ophthalmol Vis Sci* 2017;58:5993–5999. [PubMed: 29183045]
48. In JH, Lee SY, Cho SH, Hong YJ. Peripapillary Vessel Density Reversal after Trabeculectomy in Glaucoma. *Journal of ophthalmology* 2018;2018:8909714. [PubMed: 30046465]
49. Venkataraman ST, Flanagan JG, Hudson C. Vascular reactivity of optic nerve head and retinal blood vessels in glaucoma--a review. *Microcirculation (New York, NY : 1994)* 2010;17:568–81. [PubMed: 21040122]



Figure 1. Overall design of the multi-pressure dial (MPD) system used in this study. As demonstrated in “A”, each side of the goggle makes a separate seal around the periocular space and can be adjusted to a specific target pressure that is independent from the contralateral side. “B” shows the location of small holes (yellow arrow) drilled in the medial sides of the goggle that enables clear anterior surface of the lens during the imaging procedure.

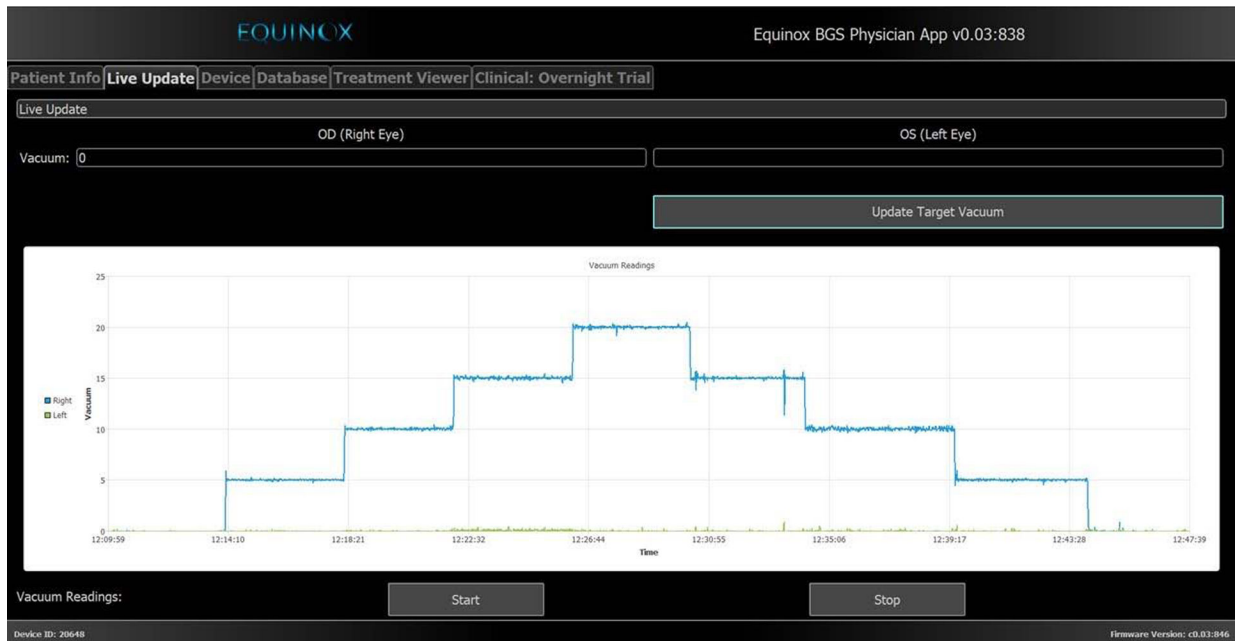


Figure 2.

The Equinox software enables to set separate user defined target pressures and allows for real-time tracking of the negative pressure inside each periorcular space. This figure shows a representation of the methodology used in this study. After making a perfect periorcular seal around the target eye of each participant, the periorcular pressure was set at different levels starting from 0 mmHg and then lowered at increments of 5 mmHg to a maximum of -20 mmHg. After that, the target pressure was increased at increments of 5 mmHg back to the baseline. Images were taken after 2 minutes at each target pressure to allow for stabilization of the measurements.

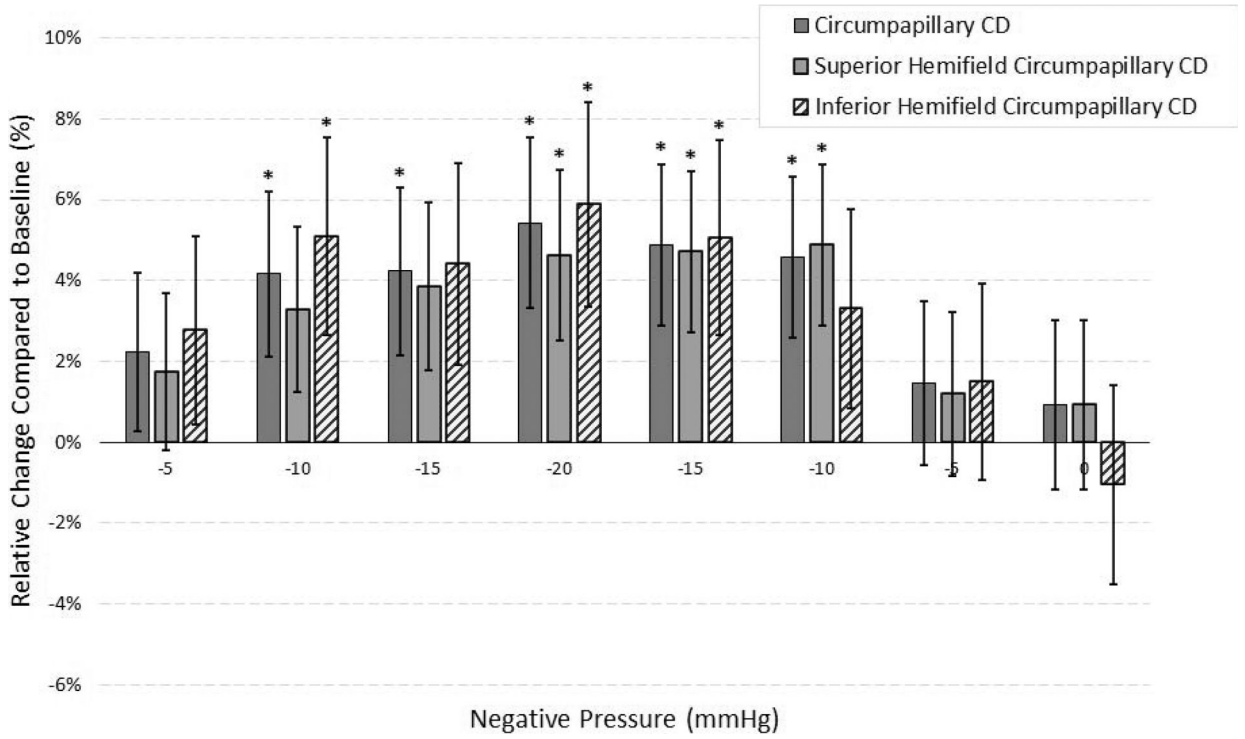


Figure 3. Mean (\pm standard error) relative changes of global and hemifield circumpapillary capillary density (CD) measurements compared to their respective baseline values at different levels of negative pressure. The “*” sign indicates statistically significant (P -value < 0.05) changes.

Table 1.

Ramp-Up and Ramp-Down Schedule of the Imaging Protocol

Variable	Target Negative Pressure								
	Ramp-Up					Ramp-Down			
	Baseline	Dose 1	Dose 2	Dose 3	Dose 4	Dose 5	Dose 6	Dose 7	Dose 8
	0 mmHg (2')	-5 mmHg (2')	-10 mmHg (2')	-15 mmHg (2')	-20 mmHg (2')	-15 mmHg (2')	-10 mmHg (2')	-5 mmHg (2')	0 mmHg (2')
Circumpapillary RNFL thickness	X	X	X	X	X	X	X	X	X
Circumpapillary CD	X	X	X	X	X	X	X	X	X

RNFL: retinal nerve fiber layer, CD: capillary density.

Author Manuscript

Author Manuscript

Author Manuscript

Author Manuscript

Table 2.

Demographic and Ocular Characteristics of the Study Population (N=24)

Variables	
Age (years)	71.0 (67.7, 74.2)
Gender (Female, %)	13 (54%)
Race (Caucasian, %)	18 (75%)
IOP (mmHg)	17.46 (15.92, 18.99)
CCT (μm)	530.6 (512.8, 548.4)
Axial length (mm)	24.7 (24.0, 25.4)
Spherical Equivalent of Refraction (D)	-2.18 (-3.39, -0.97)
MD (dB)	-2.80 (-3.88, -1.72)
PSD (dB)	3.99 (2.60, 5.38)

IOP: intraocular pressure, CCT: central corneal thickness, D: diopter, MD: mean deviation, PSD: pattern standard deviation.

Results are shown in mean (95% confidence interval) for numerical variables and No. (%) for categorical variables.

Table 3.

Serial Changes of Circumpapillary RNFL Thickness and CD Compared to the Baseline Measurements
(Negative Pressure = 0 mmHg, N = 24 eyes)

Negative Pressure (mmHg)	RNFL thickness (μm) change (95% CI)	<i>P</i> value*	CD (%) change (95% CI)	<i>P</i> value*
-5	0.07 (-1.36, 1.50)	0.922	0.93 (-0.66, 2.53)	0.251
-10	-1.18 (-2.68, 0.33)	0.126	1.74 (0.07, 3.42)	0.042
-15	-0.86 (-2.39, 0.67)	0.273	1.77 (0.07, 3.48)	0.042
-20	-1.05 (-2.60, 0.51)	0.188	2.27 (0.54, 4.01)	0.010
-15	-0.88 (-2.34, 0.58)	0.238	2.05 (0.41, 3.68)	0.014
-10	0.20 (-1.27, 1.66)	0.793	1.92 (0.29, 3.55)	0.021
-5	-0.40 (-1.89, 1.09)	0.600	0.62 (-1.05, 2.28)	0.468
0	-0.33 (-1.87, 1.21)	0.674	0.38 (-1.33, 2.10)	0.661

RNFL: retinal nerve fiber layer, CD: capillary density.

Linear mixed effects model with repeated measures was used to evaluate the statistical significance.

* Statistically significant *P* values (< 0.05) are shown in bold.

Table 4.

Serial Changes of Superior Hemifield Circumpapillary RNFL Thickness and CD Compared to the Baseline Measurements (Negative Pressure = 0 mmHg, N = 24 eyes)

Negative Pressure (mmHg)	RNFL thickness (μm) change (95% CI)	<i>P</i> value*	CD (%) change (95% CI)	<i>P</i> value*
-5	0.00 (-2.19, 2.19)	> 0.99	0.74 (-0.87, 2.35)	0.366
-10	-1.78 (-4.08, 0.52)	0.129	1.39 (-0.30, 3.08)	0.107
-15	-1.16 (-3.50, 1.18)	0.332	1.62 (-0.10, 3.34)	0.064
-20	-1.56 (-3.94, 0.82)	0.198	1.95 (0.20, 3.70)	0.029
-15	-1.31 (-3.55, 0.93)	0.251	1.99 (0.34, 3.63)	0.018
-10	-0.06 (-2.30, 2.18)	0.957	2.06 (0.42, 3.70)	0.014
-5	-0.71 (-3.00, 1.57)	0.540	0.50 (-1.17, 2.18)	0.555
0	-0.95 (-3.30, 1.41)	0.430	0.39 (-1.34, 2.12)	0.656

RNFL: retinal nerve fiber layer, CD: capillary density.

Linear mixed effects model with repeated measures was used to evaluate the statistical significance.

* Statistically significant *P* values (< 0.05) are shown in bold.

Table 5.

Serial Changes of Inferior Hemifield Circumpapillary RNFL Thickness and CD Compared to the Baseline Measurements (Negative Pressure = 0 mmHg, N = 24 eyes)

Negative Pressure (mmHg)	RNFL thickness (μm) change (95% CI)	<i>P</i> value*	CD (%) change (95% CI)	<i>P</i> value*
-5	0.13 (-2.23, 2.49)	0.912	1.15 (-0.74, 3.05)	0.232
-10	-0.48 (-2.96, 2.00)	0.702	2.11 (0.12, 4.10)	0.037
-15	-1.05 (-3.57, 1.48)	0.416	1.83 (-0.19, 3.85)	0.076
-20	-1.10 (-3.67, 1.47)	0.401	2.44 (0.38, 4.50)	0.020
-15	-0.62 (-3.07, 1.83)	0.619	2.10 (0.14, 4.06)	0.036
-10	-0.43 (-2.92, 2.06)	0.735	1.37 (-0.62, 3.36)	0.177
-5	-0.57 (-3.03, 1.89)	0.651	0.62 (-1.35, 2.60)	0.535
0	-2.39 (-4.89, 0.11)	0.061	-0.43 (-2.44, 1.57)	0.671

RNFL: retinal nerve fiber layer, CD: capillary density.

Linear mixed effects model with repeated measures was used to evaluate the statistical significance.

* Statistically significant *P* values (< 0.05) are shown in bold.